Cell, Vol. 107, 477–487, November 16, 2001, Copyright ©2001 by Cell Press

Microarray Identification of FMRP-Associated Brain mRNAs and Altered mRNA Translational Profiles in Fragile X Syndrome

Victoria Brown,[1,2,7] Peng Jin,[1,2,7] Stephanie Ceman,[1,2] Jennifer C. Darnell,[4] William T. O'Donnell,[1,2] Scott A. Tenenbaum,[5] Xiaokui Jin,[2] Yue Feng,[3] Keith D. Wilkinson,[2] Jack D. Keene,[5] Robert B. Darnell,[4] and Stephen T. Warren[1,2,6]

[1]Howard Hughes Medical Institute
Department of Human Genetics
Department of Pediatrics
[2]Department of Biochemistry
[3]Department of Pharmacology
Emory University School of Medicine
Atlanta, Georgia 30322
[4]Laboratory of Molecular Neuro-Oncology
The Rockefeller University
New York, New York 10021
[5]Department of Microbiology
Duke University Medical Center
Durham, North Carolina 27710

Summary

Fragile X syndrome results from the absence of the RNA binding FMR protein. Here, mRNA was coimmunoprecipitated with the FMRP ribonucleoprotein complex and used to interrogate microarrays. We identified 432 associated mRNAs from mouse brain. Quantitative RT-PCR confirmed some to be >60-fold enriched in the immunoprecipitant. In parallel studies, mRNAs from polyribosomes of fragile X cells were used to probe microarrays. Despite equivalent cytoplasmic abundance, 251 mRNAs had an abnormal polyribosome profile in the absence of FMRP. Although this represents <2% of the total messages, 50% of the coimmunoprecipitated mRNAs with expressed human orthologs were found in this group. Nearly 70% of those transcripts found in both studies contain a G quartet structure, demonstrated as an in vitro FMRP target. We conclude that translational dysregulation of mRNAs normally associated with FMRP may be the proximal cause of fragile X syndrome, and we identify candidate genes relevant to this phenotype.

Introduction

Fragile X syndrome is a common cause of mental retardation that results from a deficiency of the fragile X mental retardation protein, FMRP (Jin and Warren, 2000). FMRP is encoded by *FMR1*, an X-linked gene that harbors a $(CGG)_n$ trinucleotide repeat in its 5′ untranslated region. In most patients, this repeat undergoes expansion that leads to transcriptional silencing of the *FMR1* gene (Verkerk et al., 1991; Oberle et al., 1991; Sutcliffe et al., 1992).

FMR1 and its autosomal paralogs, the *f*ragile *X*-*r*elated genes *FXR1* and *FXR2*, encode a small family of RNA binding proteins that share over 60% amino acid identity (Ashley et al., 1993; Siomi et al., 1993, 1994; Zhang et al., 1995). As an RNA binding protein, FMRP has been shown to bind to RNA homopolymers as well as a subset of brain transcripts in vitro (Ashley et al., 1993; Brown et al., 1998).

FMRP is largely cytoplasmic, incorporated into large messenger-ribonucleoprotein (mRNP) particles (Eberhart et al., 1996; Feng et al., 1997a, 1997b; Khandjian et al., 1996; Tamanini et al., 1996). The FMRP-mRNP complex is composed of several proteins including other RNA binding proteins such as FXR1P and FXR2P (Bardoni et al., 1999; Ceman et al., 1999, 2000; Schenck et al., 2001). Purified FMRP displays an intrinsic RNA binding capacity (Brown et al., 1998), and in the cytoplasm, FMRP-mRNP is associated with translating polyribosomes (Eberhart et al., 1996; Feng et al., 1997a; Khandjian et al., 1996; Tamanini et al., 1996). A missense mutation in the second KH domain of FMRP (I304N), which results in a severe fragile X phenotype, prevents this polyribosome association, suggesting that the FMRP association with polyribosomes is functionally important (De Boulle et al., 1993; Feng et al., 1997a).

A hypothesis has been posited that when FMRP is absent, the mRNAs normally associated with FMRP-mRNP complexes may be translationally misregulated, which, in the brain, leads to cognitive deficits (Jin and Warren, 2000). To test this hypothesis, we have used microarrays to identify mRNAs that are selectively associated with FMRP-mRNP complexes in the murine brain. In a parallel approach, we also identified mRNAs that exhibit abnormal polyribosome profiles in cells derived from fragile X syndrome patients, suggesting that the absence of FMRP alters translation. Comparing these two sets of mRNAs identifies a subset of messages that associate with FMRP in vivo and display abnormal polyribosome profiles in the absence of FMRP. Moreover, many of these mRNAs contain a G quartet structure, which has been shown to be the structural target of FMRP (Darnell et al., this issue of *Cell*).

Results

Strategy to Isolate and Identify mRNAs Associated with FMRP-Containing mRNP Particles

To identify mRNAs associated with FMRP in vivo, a strategy was devised to specifically immunoprecipitate FMRP-containing mRNP particles and to identify the copurified mRNAs by probing microarrays. A similar strategy was used previously to identify mRNA targets of the ELAV/Hu neuronal protein, HuB (Tenenbaum et al., 2000). For murine FMRP, a monoclonal antibody (mAb 7G1-1) was developed by immunizing the *Fmr1* knockout (KO) mice with mouse FMRP (Brown et al., 1998). The epitope recognized by mAb 7G1-1 was mapped to a region of nonhomology with the *Fxr1* and *Fxr2* proteins (Figure 1A). Immunoprecipitations from

[6]Correspondence: swarren@emory.edu
[7]These authors contributed equally to this work.

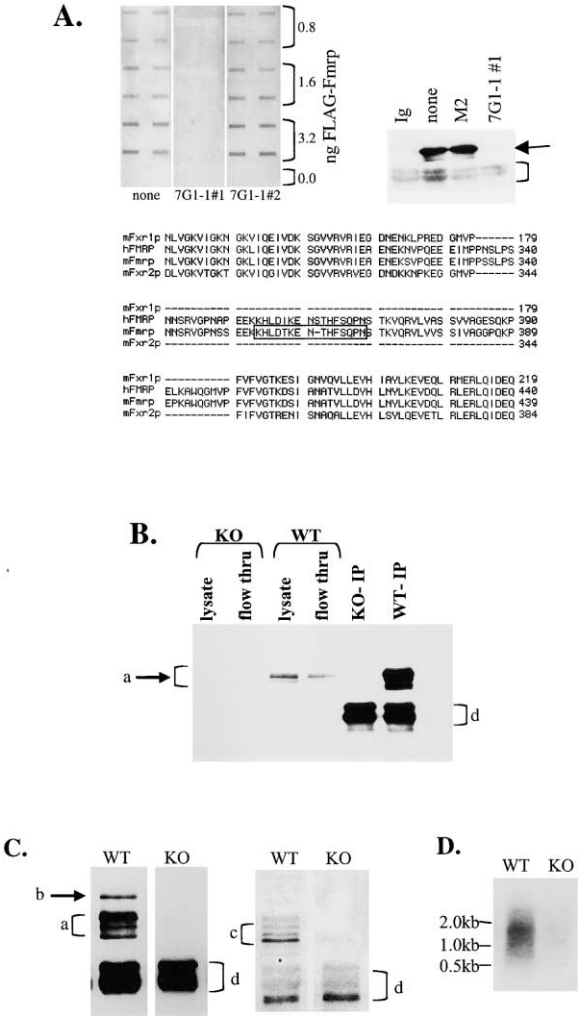

Figure 1. Immunoprecipitation of the FMRP-mRNP Complex

(A) Left: Competitive Western blot analyses were performed with purified FLAG-FMRP and probed with 7G1-1 antibody mixed with the indicated peptide competitors at 1000 × molar excess. The labels mean the following: none, no peptide; 7G1-1 #1, $_{354}$KHLDTKENTHFSQPN$_{368}$; and 7G1-1 #2, $_{367}$PNSTKVQRVLVSSIV$_{382}$. Right: Peptide 7G1-1 #1 blocks immunoprecipitation of FMRP. Lysates prepared from the FLAG-FMRP-expressing L-M cells (Ceman et al., 1999) were immunoprecipitated with 7G1-1 that was untreated (none), preincubated with the irrelevant FLAG M2 peptide (M2), or preincubated with the peptide 7G1-1 #1 (7G1-1 #1). Antibody matrix alone is shown in the lane marked Ig. Precipitates were probed with the 1C3 anti-FMRP antibody. FMRP is indicated by the arrow; antibody chains are indicated by the bracket. Bottom: Partial protein alignment of human (h) and murine (m) Fmr and Fxr proteins. mAb 7G1-1 recognize the boxed amino acids 354–368 of mFMRP, in a region with no homology to the Fxr paralogs.

(B) Whole brain lysates were prepared from wt or *Fmr1* KO mice, immunoprecipitated with the mAb 7G1-1, and probed with the 1C3 anti-FMRP antibody. The labels mean the following: lysate, input; flow thru, unbound; and IP, immunoprecipitated material. (a) indicates FMRP isoforms, and (d) indicates antibody chains.

(C) Paralogs, FXR2P and FXR1P coprecipitate with FMRP. The left panel shows probing with (a) anti-FMRP antibody (1C3), and (b) anti-FXR2P antibody (A42). A separate aliquot was probed with anti-Fxr-1 antiserum (right panel, c).

(D) FMRP associates with poly(A)$^+$ RNA in mouse brain. Immunoprecipitations were performed from wt and KO brain lysates, RNA was extracted, and first strand cDNA was generated and visualized by autoradiography.

whole brain lysates of wild-type (wt) and KO sibling mice (congenic on the C57Bl/6J strain) revealed that the antibody efficiently immunoprecipitates at least three of the predominant FMRP isoforms (Figure 1B, a). Although the antibody does not immunoprecipitate the Fxr proteins from KO brains (Figure 1C, lanes KO), both FXR1P and FXR2P were found associated with FMRP in wt mouse brain (Figure 1C, lanes WT, b and c), demonstrating the immunoprecipitation of the mRNP complex. Nucleic acid extraction of the immunoprecipitant and oligo dT-primed reverse-transcription showed the presence of poly(A)$^+$ RNA. Very little background RNA was found in the control immunoprecipitations from the KO brain lysates (Figure 1D).

Microarray Analysis of the Resident mRNAs in the FMRP-mRNP Complex

En masse identification of the mRNAs coimmunoprecipitated with the FMRP mRNP complex was achieved using the Affymetrix Murine Genome U74 (MG-U74) and Murine 19K (Mu19K) oligonucleotide microarrays. These arrays allowed the interrogation of 25,181 RNAs from the UniGene database and 19,021 messages from the TIGR database. For independent array screens, fresh lysates from pooled wt and from pooled KO brains (2 each) were prepared, and 20% of the total volume of each lysate was used to isolate total RNA as input RNA. The remainder of the brain lysates was subjected to 7G1-1 mAb immunoprecipitation (IP) followed by RNA extraction to isolate the IP RNA. wt-IP and KO-IP RNA samples were used to generate cRNA that was hybridized, in parallel with cRNA generated from input RNA, onto identical MG-U74 arrays. As shown in Figure 2A, the microarrays probed with input RNA exhibited bright fluorescence, consistent with the complex gene expression pattern of the murine brain. Less than 0.05% of the RNAs were substantially changed when comparing wt versus KO whole brain lysates (unpublished data), indicating that FMRP deficiency does not result in widespread mRNA changes at steady state. Consistent with earlier studies that suggested FMRP associates with only a subset of mRNAs (Ashley et al., 1993), the wt-IP microarrays showed substantial intensity loss for most of the genes found to be expressed in the input lysate. The KO-IP microarrays exhibited further intensity loss when compared to the WT-IP. Although detectable signals were evident on the KO-IP arrays, these were presumably due to background interactions with the antibody matrix, independent of FMRP.

Of the 25,181 total genes available on the MG-U74 microarray, 11,067 genes (~44%) were present in the total wt brain lysate. The analysis of the coimmunoprecipitated mRNA was carried out in two parts; first, the wt-IP mRNA profile was analyzed using the KO-IP mRNA profile as the baseline, and second, wt-IP mRNA profile was compared against the total wt input RNA profile. The former analysis presumably identifies FMRP-independent mRNAs associated with the antibody matrix, while the latter analysis identifies those mRNAs scored as present in the wt-IP relative to the wt input, discarding those mRNAs whose high abundance in the input lysate may be responsible for their presence in the IP sample. While discarding genes in either of these approaches may remove bona fide FMRP-associated messages, it

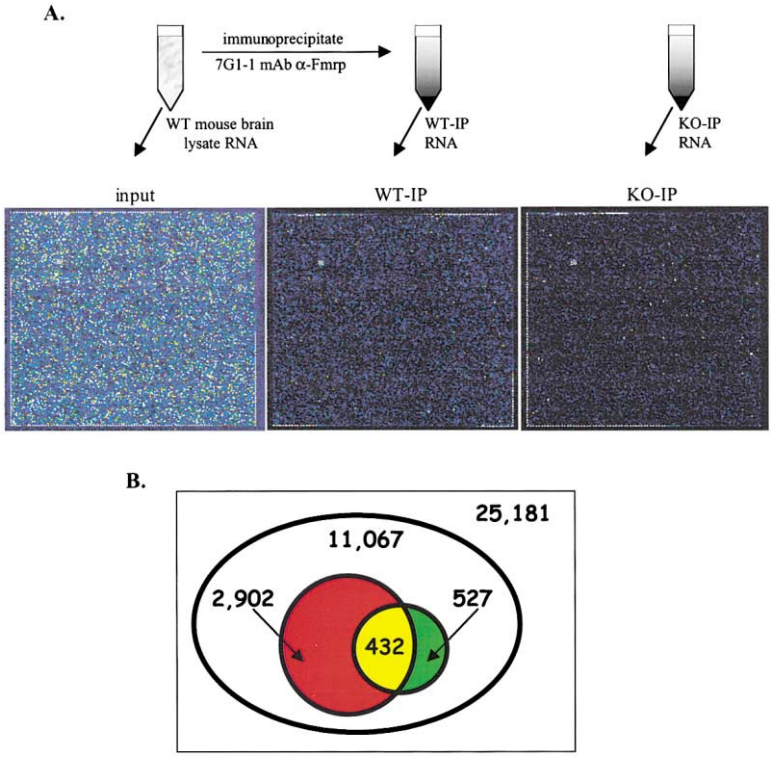

Figure 2. Analysis of the RNAs Coimmunoprecipitated with the FMRP-mRNP

(A) The MG-U74 gene chips were hybridized with cRNA generated from total RNA from wt brain input lysate (input, left panel), from RNA coimmunoprecipitated with FMRP from wt mouse brain (wt-IP, center panel), or from RNA immunoprecipitated from *Fmr-1* KO mouse brain (KO-IP, right panel).

(B) Venn diagram of the RNAs associated with the FMRP-mRNP. The square depicts the genes available on the MG-U74 chips. The white ellipse represents the genes detected in the wt brain lysate input. The red circle indicates the genes enriched in the wt-IP versus KO-IP. The green circle shows the genes enriched in the wt-IP versus the input. The yellow intersection indicates those genes enriched in the wt-IP in both analyses.

results in a relatively stringent selection and should minimize false positives. As displayed in the Venn diagram (Figure 2B, red circle), 2,902 mRNAs (26% of expressed messages) were at least 4-fold enriched in the wt-IP mRNAs when compared to the KO-IP mRNAs. However, many of these enriched mRNAs are also found at high abundance in the input lysate such that, of the 11,067 expressed genes in the total input brain lysate, only 527 mRNAs (5% of expressed messages) showed a 4-fold or greater enrichment over the input lysate by immunoprecipitation (Figure 2B, green circle). Combining these two results showed that 15% of the 2,902 genes identified in the first analysis and 82% of the 527 genes identified in the second analysis were identical and met both criteria for enrichment in the wt-IP (Figure 2B, yellow region). The intersection conservatively represents 432 genes, or 3.9% of the 11,067 expressed RNAs. This number is remarkably consistent with an earlier and much more crude estimate, suggesting that ~4% of human fetal brain messages associated with FMRP in vitro (Ashley et al., 1993).

The top 80 mRNAs enriched in the FMRP-mRNP are shown in Table 1 (full data sets available as supplemental data at http://www.cell.com/cgi/content/full/107/4/477/DC1). The genes were sorted in descending order by the "fold change" in the wt-IP versus KO-IP (baseline) comparison, and then sorted again in descending order by the fold change in the wt-IP versus input (baseline) comparison. The final rank of each probe set reflects the sum of these 2-fold change values: (wt-IP versus KO-IP) + (wt-IP versus input). The largest message enrichment in the wt-IP when compared with the KO-IP was 77-fold for a Sec7-related transcript KIAA0763, identified by homology as the guanine nucleotide exchange factor. The transcript for *SAPAP4*, encoding the PSD95-associated protein 4, had the highest wt-IP enrichment over wt input lysate, which was approximately 34-fold. The highest average difference changes of the wt-IP relative to the message prevalence in the lysate was approximately 18,000 and 14,000 for the transcript similar to *Peroxidasin* and the *Septin 3* GTPase, respectively. All transcripts ranked in the top 20 had average difference changes (versus input) in excess of 1,000.

An independent immunoprecipitation experiment was performed and analyzed with a different version of the Affymetrix murine gene chips, the Mu19K expression array. By using the same criteria as in the MG-U74 experiment, genes showing a 4-fold or greater enrichment during the immunoprecipitation were identified (full data sets available as supplemental data). When the two independent experiments were compared, 36 of the top 80 RNAs described in Table 1 were not available on the Mu19K chips, and therefore were not tested by the Mu19K data (Table 1, N/A). However, the Mu19K array data confirmed the FMRP-mRNP enrichment for 28 of the 44 genes tested (64%) (Table 1). It should be noted, however, that a number of genes were represented on both array types but with different sequences in the oligonucleotides, potentially confounding reproduction of the MG-U74 data.

Confirmation of the Association between FMRP-mRNP and the mRNAs Identified by Microarrays

To independently demonstrate that the mRNAs identified in Table 1 are associated with the FMRP-mRNP, fresh immunoprecipitations were performed in the presence of an excess of nonspecific RNA competitors, either yeast tRNA or heparin. Neither tRNA nor heparin

Table 1. Messenger RNAs Associated with the Fmrp-mRNP in Mouse Brain

		MG-U74		Mu 19K			MG-U74		MU 19K
Rank	Homology (MG-U74 Probe Set)	wtIP/KOIP Fold Chg.	wtIP/Input Fold Chg.	wtIP/Input Fold Chg.	Rank	Homology (MG-U74 Probe Set)	wtIP/KOIP Fold Chg.	wtIP/Input Fold Chg.	wtIP/Input Fold Chg.
1	Sec7-rel. GEF sim. to KIAA0763 (112719_at)	77	14.5	6.8	41	KIAA1042 prot. (96124_at)	26.1	7.3	5.6
2	Tyrosine Kin.,, AATYK (100994_at)	52.4	12.7	N/A[a]	42	Rho-interact. P116 RIP (94899_at)	26.7	6.6	2.7
3	iGluR, kainate-R 5γ2, Grik5 (104409_at)	41.8	21.4	N/A	43	Rab3-assoc.GEF, sim. to MADD (105258_at)	18.9	14	10.1
4	Brain Angiogen. Inh., BAI2 (106947_at)	43.6	19.3	4.4	44	MHC H2-K(114777_i_at)	28.6	4.2	2
5	PSD-95 assoc.SAPAP4, KIAA0964 (104136_at)	28.4	33.8	6.7	45	Celera mRNA hCT8410 (104105_at)	21.1	10.3	14.6
6	Zn. finger Mtsh-1 (106265_at)	50.4	11.6	7.5	46	Na^+channel-related prot.(97387_at)	25.5	5.8	2.1
7	murine Unc13-like prot. (110722_at)	50.1	11.1	N/A	47	PI 4 kin., p230 (104208_at)	17.4	13.9	5.5
8	Arf GTPase activator, GIT1 (97339_at)	22.5	33.7	1.8	48	Msx2-BP, Mint (110008_at)	26.6	4.6	N/A
9	Pumilio 2 (112390_at)	49.3	5.5	4.2	49	Spectrin β3, Spnb3 (93618_at)	21.6	9.3	N/A
10	K^+ channel HCN2, HAC1 (94194_s_at)	25.1	27.8	N/A	50	Celera mRNA hCT28708(112918_at)	23.5	6.7	N/A
11	sim. to DAP-1 and SAPAP3 (116746_at)	46.8	5.1	N/A	51	hCT25324,Ub-lig.-like(109944_at)	16.7	13.5	4
12	GAP-assoc. p190 (96208_at)	29.7	22.1	11.9	52	Celera mRNA hCT25324 (92958_at)	20.6	9.4	4.3
13	KIAA0284 sim. to Septin 3 GTPase (131216_f_at)	23.5	27.1	N/A	53	Patched-related prot.(104030_at)	21.5	8.4	N/A
14	sim. to KIAA0561 (104032_at)	20.4	29.6	15.8	54	KIAA0633 prot. (108712_at)	25.3	4.6	N/A
15	G prot. effector, GRIN1, Z16 (113864_at)	27.2	22.2	N/A	55	Celera mRNA hCT33144 (108765_at)	22.5	7.2	13.7
16	sim. to PS1-BP, p0071, plakophilin4 (96187_at)	35.4	12.6	9.5	56	NAG-6-O-sulfotrans. (102639_at)	22.3	7.3	5.9
17	KIAA0918, TOLL-related prot. (107354_at)	40.5	6.3	N/A	57	MAPK4, p63 (140436_at)	22	7.6	N/A
18	KIAA0602, ribosomal S7 prot. (111873_at)	37.7	7.3	9.6	58	Zn. finger Rantes(103369_at)	18.5	11	3.3
19	Zn. finger Friend of GATA1, FOG (97974_at)	16.9	27.7	1.9	59	OCAM-GPI precusor; NCAM2 (96518_at)	15.8	13.7	N/A
20	sim. to 5′AMP-activ'd kinase (139527_at)	25.7	18.9	N/A	60	2-Oxoglutarate dehydrog'se (96879_at)	25	4.4	12.4
21	Inositol 1,4,5 triphos. recept. p400 (94977_at)	37.3	4.7	1.9	61	a-Latroxin receptor (112497_at)	23.2	6.2	4.4
22	Rab6-assoc. GDI (104108_at)	34.8	6.5	6.6	62	SNF1-related kinase (97429_at)	18.8	10.3	4.9
23	pBR140, Peregrin (114619_at)	33.6	7	13.5	63	Celera mRNA hCT19890(103316_at)	16.2	12.9	N/A
24	Nuclear P'tse, dsPTP, myotubularin-rel. (111847_at)	25.8	14.7	1.2	64	sim. to MKP-1, -L, & -6 dusPTP'tase (133560_at)	14.1	15	N/A
25	DM prot., DMR-D9(96193_at)	19.5	20	1	65	Celera mRNA hCT33304(102969_at)	23.1	5.9	N/A
26	Celera mRNA hCT8453 (104299_at)	31.4	7.6	N/A	66	sim. to Myotubularin (104427_at)	14.2	14.6	1.6
27	Steroid recept. Co-activator le (106920_at)	32.6	6.4	9.8	67	Celera mRNA hCT13240(130936_f_at)	11.9	16.9	N/A
28	Hsp75-like TNF1R-assoc. prot. (95886_g_at)	21.8	17.1	2.9	68	PI 3 kin.,reg. subu. P85b, Pik3r2 (102759_at)	21.6	7.1	6.9
29	sim. to Interleukin-enhancer-BF1 (95596_at)	19.8	17.9	1.1	69	Vav-related KIAA1626 (112513_at)	13.9	14.8	N/A
30	sim. to Adenylate Cyclase 5&6 (138967_i_at)	18.1	19.3	N/A	70	Casein kin. Ig2 (96284_at)	24.4	4.2	5.6
31	L-type Ca^{2+} chan. B3, Cacnb3 (98483_at)	31.8	5.3	2.4	71	Zn. finger Png-1; myelin Mytl1 (96496_g_at)	11.5	16.6	N/A
32	Celera mRNA hCT12896;KIAA0701 (109149_at)	30.8	5.2	8.3	72	sim. to Tensin (110429_at)	23.4	4.1	N/A
33	sim. to MAP1A and MAP1B (116100_f_at)	29.1	6.3	4.5	73	sim. to Synaptotagmin-related prot. (93821_at)	16.4	11	N/A
34	Testis prot. Kin., Tesk1 (102033_at)	19.6	15.3	2	74	M-RdgB2 (139194_at)	20	7.3	N/A
35	KIAA0306, Pro.-rich MP-3, PRP3 (96725_at)	24.6	9.9	2.8	75	Tyrosine Kin., Ack; Cdc42 (102850_at)	15.9	11.1	2.7
36	Celera hCT14692 sim. to KIAA1246 (131226_at)	17.3	17	N/A	76	sim. to TMEM1 (104202_at	20	6.9	N/A
37	sim. to KIAA0918 prot. (134810_s_at)	11.7	22.6	N/A	77	sim. to Link GEF II (105927_at)	13.2	13.6	N/A
38	Celera mRNA hCT7158 (103736_at)	27.9	6.3	N/A	78	sim. to Acetylglucosaminyl transf se (103276_at)	21.1	5.4	N/A
39	Circ. Rhythm prot., SCOP, KIAA0606 (109399_at)	29.5	4.6	8.7	79	Down syndr.cell adhes. molec., Dscam (116463_at)	13.2	13.3	N/A
40	Celera mRNA hCT9545(106009_at)	27.1	6.4	N/A	80	sim. to D.melanogaster Peroxidasin (130534_i_at)	19.1	7.3	N/A

Probe sets are ranked by the sum of the fold change values [(wt-IP versus KO-IP) + (wt-IP versus Input)] determined by MG-U74 microarray analysis.

[a]N/A denotes Fmrp-mRNP-associated RNAs determined by MG-U74 not represented on the Mu19K chips.

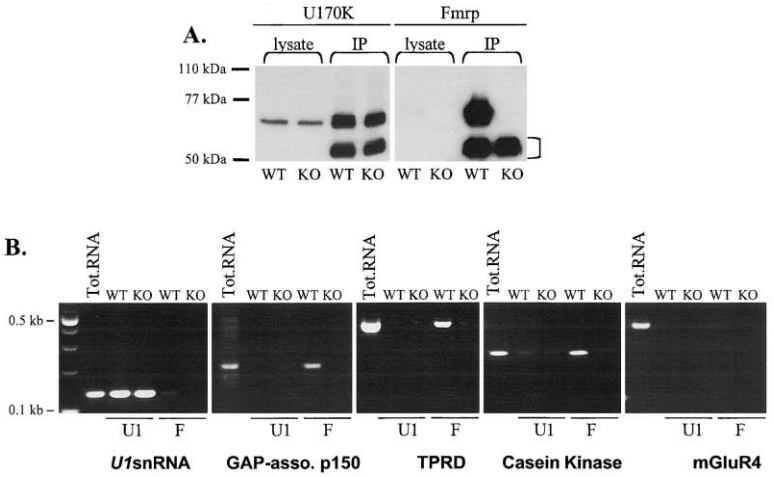

Figure 3. FMRP-mRNP Associated RNAs Are Specific to the FMRP-Containing Complex

(A) Immunoprecipitations from mouse brain lysates were performed with anti-U1-70Kp antibody (left panel) or anti-FMRP 7G1-1 antibody (right panel). Western blots of immunoprecipitates were probed with antibody against the U1-70K protein (left panel) or the 1C3 antibody against the FMRP protein (right panel). "Lysate" indicates input brain lysates; "IP" indicates immunoprecipitated proteins. The bracket at right indicates the antibody chains.

(B) Examples of RT-PCR analyses of the anti-U1-70K and anti-FMRP immunoprecipitations. RNA was purified from the immunoprecipitates above and reverse transcribed prior to the PCR. "Tot.RNA" indicates wt mouse brain total RNA, "U1" indicates the anti-U1-70K immunoprecipitations, and "F" indicates the analysis of the anti-FMRP immunoprecipitations. DNA molecular weight standard is shown at left. PCR primers used are (left to right) *U1*snRNA, GAP-associated protein *190*, murine *TPRD*, Casein Kinase *CK1g2*, and mGluR4, an unbound control.

abrogated the specific RNA association with the FMRP-mRNP for a random group of messages from Table 1 (data not shown). We next asked if an RNA ligand that copurifies with another RNP would be present in the FMRP-mRNP. The U1-70K small nuclear RNP (snRNP) is a splicing complex that specifically binds the U1 snRNA (Query et al., 1989). This complex was immunoprecipitated from fresh wt and KO lysates with an anti-U1-70K mAb, and in parallel the FMRP-mRNP was immunoprecipitated from the same lysates (Figure 3A). The anti-U1-70K antibody efficiently precipitated the U1-70K protein from both wt and KO brain lysates, whereas the anti-FMRP 7G1-1 antibody precipitated FMRP, as expected, only from the wt brain lysate. The RNA recovered from each precipitation was analyzed by RT-PCR (Figure 3B). For each gene of interest, the primer pairs were also tested in a RT-PCR reaction with 0.1 μg of total brain RNA (Figure 3B, Tot.RNA). The U1snRNA, previously determined to be the U1-70K ligand, was enriched in the U1-70K precipitates from both wt and KO mouse brain. However, this same RNA was not found in substantial amounts in the FMRP precipitate (Figure 3B). In contrast, the eight tested FMRP-associated mRNAs were only found in the FMRP precipitates from wt mouse brain and not in the U1-70K precipitates nor in the control anti-FMRP immunoprecipitation from KO brain (Figure 3B and data not shown). In a set of random mRNAs that were not enriched in the FMRP-mRNP microarray studies, including the neuronal *mGluR4, Dynamin*, and *Homer* messages, none were detected in either the U1-70K or FMRP complexes (Figure 3B and data not shown).

To further confirm the microarray data, we performed quantitative LightCycler RT-PCR analysis by using RNAs from wt-IP and wt input. As shown in Table 2, of three tested mRNAs that were not found by microarray analysis to be enriched in the wt-IP, all showed little enrichment upon LightCycler analysis. In contrast, three genes that were found in the microarray analysis to be enriched in the wt-IP, relative to wt input, were also found to be highly enriched in the IP by quantitative RT-PCR. Indeed, the *Sec7-related* gene, predicted by the microarray analysis to be highly enriched in the wt-IP, showed a greater than 60-fold enrichment in the wt-IP over the wt input by LightCycler analysis. The above experiments confirm the microarray data and demonstrate that a subset of brain mRNAs is reproducibly associated with the FMRP-mRNP complex from the mouse brain.

Altered Polyribosomal mRNA Profile in the Absence of FMRP

While the above experiments point to potential RNA ligands of the FMRP-mRNP complex, they do not address any functional attributes of this association. In an independent series of experiments, microarray analysis was again utilized, but now was used to discern any shifts in individual mRNAs, in the presence or absence of FMRP, on a sucrose gradient that fractionates messages by their relative association to ribosomes. Previous studies have shown most FMRP to be in the polyribosome fractions of cell lysates (Eberhart et al., 1996; Feng et al., 1997a; Khandjian et al., 1996; Tamanini et al., 1996). In fragile X cells, without FMRP, the FXR proteins do not substantially change their associations with polyribosome (Feng et al., 1997a). Thus, it appears that a similar mRNP may form with just the FXR proteins, although it may be hypothesized that the absence of FMRP in this complex could alter the translational profile of a subset of mRNAs. To test this hypothesis, we utilized microarrays to compare the mRNA profiles of high-molecular-weight polyribosomes between normal human cells and cells derived from fragile X syndrome patients. If changes in the translational profile of messages are observed in the absence of FMRP, these mRNAs should (at least partially) correlate to the immunoprecipitation data if it is functionally important.

To reduce any inherent individual variation that is unrelated to FMRP, we performed sucrose gradient frac-

Table 2. Verification of Microarray Data using LightCycler Real-Time PCR

Genes	Mouse UniGene Cluster	Association with FMRP-mRNP Determined by Microarray Analysis	Scaled Fold Enrichment in wt-IP over wt-INPUT by LightCycler PCR
Similar to microsomal glutathionse S-transferase 3	Mm. 29823	No	1.87
Glutamate receptor, ionotropic, AMPA1	Mm. 4920	No	−1.83
Synaptotagmin 1	Mm. 5101	No	1.02
KIAA0317 protein	Mm. 24446	Yes	31.3
TP63	Mm. 54143	Yes	36.8
Sec7-rel. GEF similar to KIAA0763	Mm. 89798	Yes	60.5

tionation from pooled (five cell lines each) as well as from individual human lymphoblastoid cell lines, derived from either normal males or fragile X full mutation males. Consistent with previous observation (Feng et al., 1997a), in pooled normal cells, FMRP associates with polyribosomes (Figure 4A). Neither *FMR1* message nor FMRP can be detected in any of the fragile X cell lines (Figure 4A and data not shown). RNA was purified from total cytoplasmic extract (total mRNA), as well as from the high-molecular-weight polyribosome fractions (fractions 9–11, Figure 4A). cRNA was prepared for hybridization onto microarrays containing more than 35,000 human genes and/or ESTs (Affymetrix Hu35K). mRNA profiles of polyribosomal fractions from both individual and pooled fragile X cells were compared with polyribosomal fraction from either individual normal cells or pooled normal cells (baselines). In addition, expression profiles of total mRNA from pooled cells were compared to each other as well.

Overall, of >35,000 genes analyzed, ~11,000 were present, indicating that about one-third of the genes represented on the microarray are expressed in human lymphoblastoid cells. As might be expected, greater variation in gene expression was observed when the samples were derived from individual cell lines, rather than from the pooled cells (data not shown). In fragile X cells, the *FMR1* locus is transcriptionally repressed (Sutcliffe et al., 1992) and therefore serves as an ideal internal control. On the microarray, the *FMR1* mRNA was clearly present in total mRNA from normal cells but was absent in fragile X cells. In polyribosomal fractions, the *FMR1* mRNA was present in normal cells, although at a low level, but again was completely absent in fragile X cells (Figure 4C). Thus, this approach correctly identified the one known difference in mRNA expression between the normal and fragile X cells.

Overall, 144 genes from pooled fragile X cells were changed compared to pooled normal cells in the total mRNA, while 282 genes showed consistent changes in the fragile X polyribosome fractions (pooled or individual fragile X cells) compared to the normal polyribosome fraction (pooled or individual normal cells). Of these 426 genes, 31 were found in both data sets (Figure 4B). Because the alteration of a message in the total mRNA may influence the amount of that message in the polyribosome fractions, these 31 mRNAs were eliminated from further analysis. The remaining 113 genes that showed differences in total mRNA were not considered further here. Hence, we were left with 251 genes that show equivalent levels of expression in the total mRNA of pooled fragile X and normal cells but displayed consistent translational profile shift between the two cell types (i.e., the proportion of a message on high-molecular-weight polyribosomes) (Figure 4B). These genes were clustered into two groups based on whether they were increased or decreased in the polyribosomes of fragile X cells, as indicated by the shading in Figure 4B. Of the 251 genes, 136 were increased and 115 decreased in the polyribosomes of fragile X cells (full data sets available as supplemental data).

To verify these data, we performed quantitative LightCycler RT-PCR. A control gene, X-linked hypoxanthine phosphoribosyl transferase (*HPRT*), which did not show any change in either polyribosomal fractions or total mRNA on microarray analysis, was also unchanged in the RT-PCR experiments (data not shown). Consistent with microarray data, quantitative RT-PCR showed that the transcript levels of *NAP-22* and *MKPX* decreased in the polyribosomal fractions of fragile X cells while *GRP58* increased in these fractions. There was no significant change in total mRNA from any of the three genes (data available as supplemental data). To further confirm the microarray data, the distribution of *NAP-22* and *MKPX* messages in freshly prepared sucrose gradient fractions were probed by Northern blot. As shown in Figure 5, both *NAP-22* and *MKPX* were reduced in polyribosomal fractions of fragile X cells, although total cytoplasmic RNA showed no differences between normal and fragile X cells. Moreover, these data extend the microarray and LightCycler data to include gradient fractions 5–8, revealing an even more striking translational profile shift in fragile X cells, particularly for *MKPX*. Glyceraldehyde phosphate dehydrogenase (*GAPDH*), as a control, did not show any difference between normal and fragile X cells throughout the gradient or in total RNA (Figure 5). These results confirmed the selective translational profile shift of a subset of mRNA in the absence of FMRP.

Correlation of Immunoprecipitated mRNAs with Those Showing a Translational Profile Shift in Fragile X Syndrome Cells

To compare the genes associated with FMRP-mRNP in the mouse brain with the human genes exhibiting abnormal polyribosomal shift in the absence of FMRP, we searched HomoloGene database using the UniGene clusters that represented the mouse genes of interest, and we identified UniGene clusters of the human orthologs of these genes. Conversely, using the human UniGene clusters and probe set information provided by the manufacturer (EASI DATABASE v2.41, Affymetrix), the oligonucleotides that represent the murine orthologs of the human genes were also identified. Of the top 80 genes identified in mouse microarray analysis

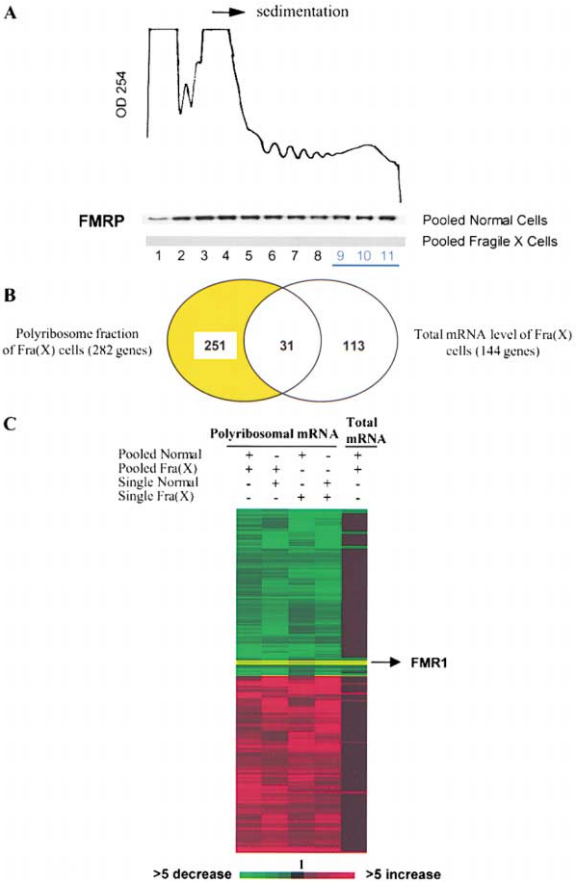

Figure 4. Comparative Analysis of mRNA Profiles from Polyribosomal Fractions and Total mRNA between Normal and Fragile X Cells

(A) Sucrose gradient fractionation of pooled normal and fragile X cells. The top panel shows the absorption profile of the sucrose gradient with the sedimentation indicated. The bottom two panels show the distribution of FMRP by Western analysis. Fraction numbers are indicated below the corresponding lanes, and fractions 9–11, used for microarray analysis, are underlined.

(B) Venn diagram of the number of genes altered in polyribosomal fractions and total lysate.

(C) Dendrogram of genes with significant changes in the polyribosome profile of patient cells. Samples used for each comparison are indicated on the top, and data from normal cells are used as baseline for all comparison. Genes that were present at higher levels in the patient cells are shown in progressively brighter shades of red, and genes that were expressed at lower levels are shown in progressively brighter shades of green. Genes shown in black were not changed. The *FMR1* gene (highlighted in yellow) is decreased in both polyribosomal fractions and total mRNA of patient cells. The identities of those genes are available from the electronic version of this manuscript at http://www.cell.com/cgi/content/full/107/4/477/DC1.

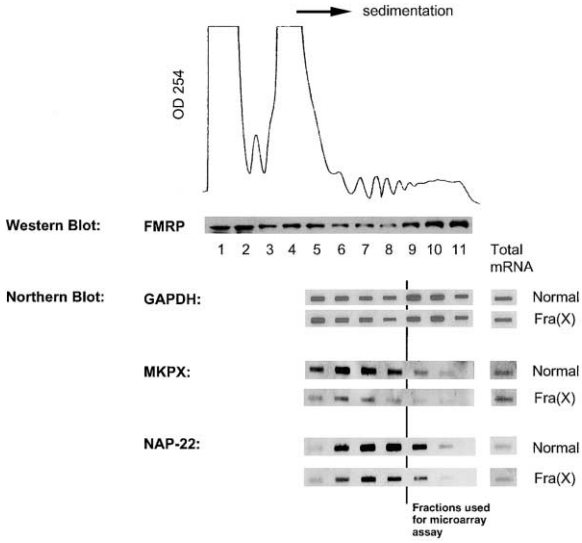

Figure 5. Northern Blot Analysis of Genes Changed in the Polyribosomal Profiles of Fragile X Cells

The top panel shows the absorption profile of sucrose gradient with the sedimentation indicated. Western blot shows the distribution of FMRP in correlation to fractions. Northern blot shows mRNA distribution from fractions 5 to 11 in the sucrose gradient, between normal and fragile X cells. An equal volume of RNA from each fraction was hybridized with different probes for selected genes, including *GAPDH* (control), *MKPX*, and *NAP-22*.

(Table 1), 48 genes are represented on the Human 35K set oligonucleotide microarray. Among these 48 genes, 28 are expressed in the human lymphoblastoid cells, and 14 (50%) were differentially associated with polyribosomes in the normal versus fragile X cells. This appears rather significant, because the entire polyribosomal mRNA profile of normal versus fragile X cells, comparing some 11,000 messages, showed only 2% of the messages as changed in the polyribosome fractions. The other 14 genes, whose messages coimmunoprecipitated with FMRP but did not exhibit abnormal polyribosomal shift, may represent mRNAs associated with the Fxr proteins, potentially revealing the speculated partial compensatory functions of the Fxr proteins. The mRNAs that differentially associated with the polyribosomes of fragile X cells and were also found in the FMRP-mRNP particle are shown in Table 3. Approximately half of these were increased (6/14) and half were decreased (8/14) in the high-molecular-weight polyribosomes of fragile X cells. Although FMRP has been shown to suppress translation of bound messages in vitro (Li et al., 2001; Laggerbauer et al., 2001), perhaps accounting for the 6 messages showing increased loading on polyribosomes in the absence of FMRP, the exact effect of FMRP on translation in vivo would appear to be more complex.

In the accompanying paper by Darnell et al. (2001 [this issue of *Cell*]), a G quartet structure was identified in vitro as the RNA target of the RGG box domain of FMRP. Of the 12 genes in Table 3 where sufficient sequence information existed for the analysis, eight (67%) genes showed the presence of a G quartet structure. Considering that only 4% of a random collection of cDNAs are predicted as possible FMRP targets, the observation that 67% of the transcripts independently determined to both immunoprecipitate with FMRP and display a translational profile shift in the absence of FMRP certainly points to the G quartet structure as being physiologically relevant in fragile X syndrome.

Discussion

Soon after the discovery of the *FMR1* gene, FMRP was recognized as an RNA binding protein, although the in vivo target RNAs have remained elusive (Ashley et al.,

Table 3. Changed mRNAs in the Fra(X) Polyribosome Fraction that also Co-immunoprecipitate with Mouse Brain Fmrp mRNP

Gene Name	Presence of G Quartet Structure	Human UniGene Cluster	Mouse UniGene Cluster	Change in the Polyribosome Fraction of Fra(X) Cells
KIAA 0964, PSD-95 assoc. SAPAP4	absent	Hs. 177425	Mm. 22094	Decrease
UNC13 (*C. elegans*)-like protein (Munc 13)	3′ UTR	Hs. 155001	Mm. 7872	Decrease
KIAA 1091, Rab6 interacting protein 1	coding region	Hs. 26797	Mm. 21904	Decrease
Similar to adenylate cyclase	unknown	Hs. 9572	Mm. 41626	Decrease
Similar to MKP-dusPTPase	absent	Hs. 29106	Mm. 46262	Decrease
TP63	3′ UTR	Hs. 137569	Mm. 54143	Decrease
Casein kinase 1, gamma 2	absent	Hs. 181390	Mm. 29873	Decrease
NAP-22	coding region	Hs. 79516	Mm. 29586	Decrease
MAP1B	5′ UTR	Hs. 103042	Mm. 36501	Increase
Similar to I38022 hypothetical protein	unknown	Hs. 10299	Mm. 24385	Increase
KIAA0929 protein, Msx2 interacting nuclear target (MINT) homolog	coding region	Hs. 184245	Mm. 25025	Increase
KIAA0317 protein	3′ UTR	Hs. 20126	Mm. 24446	Increase
Arg/Abl-interacting protein (ArgBP2)	absent	Hs. 278626	Mm. 32247	Increase
Transmembrane protein 1, TMEM1 (GT334)	3′ UTR	Hs. 94479	Mm. 27539	Increase

1993; Siomi et al., 1993). Many studies have characterized the RNA binding behavior of FMRP in vitro or in cell-free systems (Ashley et al., 1993; Brown et al., 1998; Siomi et al., 1993, 1994; Sung et al., 2000); however, the work described here identifies the repertoire of RNAs associated in vivo with the endogenous FMRP protein complex and shows translational profile changes in the absence of FMRP.

Large-Scale Identification of FMRP-mRNP-Associated mRNAs

The FMRP-immunoprecipitating mAb, 7G1-1, allows, for the first time, the purification of endogenous FMRP-mRNP complexes. The FMRP-mRNP complex was found to be associated with 3.9% of the expressed genes in mouse brain. The *Fmr1* message was not among these messages despite in vitro studies showing FMRP association with its own mRNA (Ashley et al., 1993; Brown et al., 1998). The *Fmr1* message was detected at a moderate level in the wt brain lysate, with an input (baseline) average difference value of 114 and was undetected, as expected, in KO input lysate. In comparison, 32% of the expressed genes had signal intensities higher than the *Fmr1* in the input lysate. There was a moderate 4.2-fold increase in the *Fmr1* transcript when the WT-IP RNA was compared to the KO-IP RNA (average difference change of 225), but no enrichment was found when comparing the wt-IP RNA to the wt input RNA. Although the *Fmr1* transcript may be a legitimate FMRP ligand, in light of the data presented here, it is likely there are other messages with much more avidity to this mRNP complex. Indeed, in contrast to *Fmr1*, other mRNAs were detected at extremely low levels in the wt brain lysate input yet were greatly enriched in the FMRP-mRNP. This group includes messages predicting a KIAA0561-like protein, the *Rab3* GDP/GTP exchange protein, and the Celera mRNA hCT25324, which is predicted by TBLASTX to encode an ubiquitin-ligase-like protein. In these cases, these messages were called "absent" in the input lysate. And yet, the average difference changes were 1114, 1270, and 916, respectively, in the IP versus the input, indicating substantially greater relative abundance in the immunoprecipitated mRNP.

Quantitative RT-PCR using LightCycler technology confirmed that a tested subset of transcripts predicted to be enriched by the microarray data were indeed approximately 30- to 60-fold enriched in the wt-IP relative to the wt input lysate. This included the top ranking transcript in Table 1, the *Sec7-related* guanine nucleotide exchange factor, which was confirmed in independent lysates to be approximately 61-fold enriched in the FMRP-mRNP. It should be noted however, that given the 3′ bias and the relatively short interval of cDNA sequence used in designing the oligonucleotide sequences of microarrays, false negatives occur, perhaps due to alternative splicing or to consolidation of gene family members. A case in point is the *NAP-22* transcript. On the Mu19K microarray, *NAP-22* was enriched in the wt-IP but subsequently failed to be scored highly on the MG-U74 microarray. After noting that *NAP-22* displays a translational profile shift in the absence of FMRP, the association of the *NAP-22* transcript with the FMRP-mRNP was reinvestigated using quantitative RT-PCR and was shown to be 63-fold enriched in the wt-IP relative to the total brain lysate. Since the newer MG-U74 microarray used EST-derived sequence to develop different oligonucleotides than those used in the Mu19K microarray, it is probable the two microarrays may be assaying different isoforms or family members for some genes. While it is likely the number of such genes is not high, this discrepancy, along with our relatively high stringency of analysis, suggests that we are somewhat underestimating the number of transcripts associated with the FMRP-mRNP.

Altered Polyribosomal-Association of mRNAs in the Absence of FMRP

It has been hypothesized that FMRP may be incorporated into an mRNP-complex with its mRNA ligands and, in turn, associate with translating polyribosomes, somehow modulating the translation of those mRNA ligands (Jin and Warren, 2000). Using microarrays, we have now identified a subset of mRNAs that are altered

in the high-molecular-weight polyribosome fraction of fragile X cells, most of which (251 out of 282) did not change in abundance in the total mRNA. These changes may imply an alteration in translation regulation in the absence of FMRP. Considering that synaptic abnormalities have been reported in both fragile X syndrome patients and the *Fmr1* knockout mouse, it is of substantial interest that several of the mRNAs that exhibited an abnormal polyribosome shift in fragile X syndrome cells are involved in neuronal plasticity and development/maturation of synapses, including *NAP-22*, neuritin, synaptosomal-associated protein 23, *MAP1B*, *UNC13*-like protein, and SAPAP4 (Aravamudan et al., 1999; Augustin et al., 2001; Caroni, 1997; Edelmann et al., 1996; Frey et al., 2000; Hinton et al., 1991; Naeve et al., 1997; Nimchinsky et al., 2001; Takeuchi et al., 1997).

FMRP-Specific mRNA Ligands and a G Quartet Structure

Comparing the genes identified in the complementary approaches, we find that only 2% of the expressed genes surveyed showed a translational profile shift in the absence of FMRP, yet 50% of the mRNAs that are both found in the FMRP-mRNP complex and expressed in human cells belong to this group. Because we immunoprecipitated from mouse brain (since the 7G1-1 mAb does not recognize human FMRP) and did the translational studies in human cells (since polyribosome profiles are problematic from brain tissue), there were some limitations in the comparison of the data sets, due to tissue-specific expression and species-specific microarrays. However, the data strongly support the notion that the FMRP-mRNP complex recognizes specific mRNAs and modulates their translation on polyribosomes.

We have hypothesized that RNA binding proteins in mRNP complexes interact with specific *cis* elements in a subset of mRNAs, allowing the transcripts to be regulated at the posttranscriptional level (Keene, 2001; Tenenbaum et al., 2000). This hypothesis predicts that one or more structural elements may be in common among a set of mRNAs found in mRNP complexes. Indeed, such a structural element, in the form of a G quartet, has been identified in FMRP RNA ligands by Darnell et al. (2001 [this issue]). It is remarkable that 67% of the transcripts that both immunoprecipitate with the FMRP-mRNP complex in the mouse brain and display a translational profile shift in the patient cells are predicted to contain a G quartet structure. Indeed, Darnell et al. (2001 [this issue]) has found that 11 messages in Table 3 bind to FMRP in vitro with affinities ranging from 194 nM to 599 nM. Moreover, the top-ranked *Sec7-related* guanine nucleotide exchange factor (Table 1) is predicted to have a strong G quartet structure, binds FMRP in vitro with an affinity of 322 nM, and shows Li^+ binding sensitivity, indicative of a G quartet element (Darnell et al., 2001 [this issue]). In addition, we have tested messages predicted by Darnell et al. to be FMRP ligands and have observed that two candidates examined (*ID3* and *V1a receptor*) were both enriched in the FMRP immunoprecipitates from mouse brain. Of four candidates in humans, two (*semaphorin 3F* and, again, the *V1a receptor*) were decreased in the polyribosome fractions of patient cells (5.5- and 2-fold, respectively) but were unchanged in their total RNA abundance in cytoplasmic lysates (supplemental data available). These observations strongly imply that the G quartet structure is biologically relevant to fragile X syndrome.

FMRP mRNA Ligands and the Pathogenesis of Fragile X Syndrome

The above results suggest that roughly 4% of brain transcripts are possible targets for FMRP. Given the relatively subtle features of fragile X syndrome, it might be considered surprising that the translational alteration of such a substantial number of messages does not lead to a more severe phenotype. However, it may be only a smaller subset of mRNAs, perhaps those with the greatest binding affinity to FMRP, are most influenced by the absence of FMRP. In addition, the translational profile shifts seen in the absence of FMRP does not completely remove the affected transcripts from the polyribosomes. Accordingly, it would be expected that some of the encoded protein of the affected transcripts would still be produced. Thus, the consequence of the absence of FMRP may indeed be a rather subtle cellular effect, perhaps most damaging in sensitive regions of localized protein synthesis such as in neuronal processes.

The identified transcripts reported above encode a myriad of proteins involved in neuronal function. The top-ranked probe set is the mouse ortholog of the human transcript for the *Sec7-related* guanine nucleotide exchange factor (Jackson and Casanova, 2000; Mayer et al., 2001). Sec7 domain-containing proteins, Munc13 (a family of phorbol ester receptors), and ARF (an ADP-ribosylation factor) are all involved in Golgi vesicle maturation and vesicle transport in neurons (Augustin et al., 2001; Neeb et al., 1999). Similarly, many of the other messages found (Table 1) associated with the FMRP-mRNP complex compose an interesting mix of novel messages and those whose encoded functions are intriguing in light of fragile X syndrome. For example, messages encoding proteins such as SAPAP4, DAP-1, and the kainate receptor were enriched in the FMRP immunoprecipitation, and these proteins are found closely associated with the postsynaptic density and are involved in maintaining the PSD structure and neuronal cell signaling (El-Husseini et al., 2000; Paschen et al., 1994; Satoh et al., 1997; Takeuchi et al., 1997). Recent studies showing abnormal maturation and arborization of hippocampal neurons from *Fmr1* KO mice and fragile X patients are consistent with the altered translation of these and other postsynaptic proteins (Braun and Segal, 2000; Hinton et al., 1991; Nimchinsky et al., 2001; Weiler et al., 1997). One of the next challenges generated from these data is to determine which candidate mRNAs are *most* critical to fragile X pathophysiology. The data reported here provide the necessary ingredients for further inquiry into the molecular basis of this frequent form of cognitive deficiency. Moreover, given the phenotypic overlap between fragile X syndrome and other neuropsychiatric disorders such as autism and attention deficit/hyperactivity, the mRNAs identified here may be considered a cache of candidate genes for these disorders as well.

Experimental Procedures

Antibodies

Monoclonal antibody 7G1-1 was generated by immunizing *Fmr1* knockout mice (The Dutch-Belgian Fragile X Consortium, 1994) with hexahistidine-tagged FMRP (Ceman et al., 2001). The FMRP-epitope recognized by 7G1-1 was identified by screening an expression library prepared from a partial exonuclease/DNase digestion of the *Fmr1* cDNA cloned into Novatope vector (Novagen). Competitive Western blot and immuoprecipitation were done to confirm the epitope. The extensive description of these protocols is published online as supplemental data. The 1C3 anti-FMRP was provided by Dr. J.-L. Mandel (Institute of Genetics, Illkirch, France), anti-FXR2P (A42) was a gift from Dr. G. Dreyfuss (University of Pennsylvania), anti-FXR1P antiserum was provided by Dr. A. Hoogeveen (Erasmus University, Rotterdam, Netherlands), and anti-FLAG M2 was from Sigma-Aldrich.

Mouse Brain Lysate Immunoprecipitation and Analysis

Whole brains from adult wt and *Fmr1* congenic C57Bl/6J littermates were harvested and homogenized in 2 ml/brain ice-cold buffer (10 mM Hepes [pH 7.4], 200 mM NaCl, 30 mM EDTA, and 0.5% Triton X-100) with 2× complete protease inhibitors (Boehringer-Mannheim) and 400 U/ml rRNAsin (Promega) (Ishizuka et al., 1999). All further manipulations of the brain lysates were performed at 4°C. After pelleting nuclei, the supernatants were raised to 400 mM NaCl and clarified. The resulting supernatant was precleared, and an aliquot (20%) of precleared supernatant ("input") was saved for RNA extraction. The remaining lysate was immunoprecipitated with 7G1-1 mAb (see supplemental data). The immunoprecipitate was resuspended in DEPC-treated water for protein analysis and RNA extraction.

Linear Sucrose Gradient Fractionation

Linear sucrose gradient fractionation was performed as described (Feng et al., 1997a). EBV-transformed human lymphoblastoid cell lines including normal cells (J1, AP107, CM15A, EuH154, and TN7) and fragile X cells (GM3200A, NB118, GM07294, OS9, and KJH172) were cultured at 37°C with the density of $5 \times 10^5 \approx 1 \times 10^6$/ml. After incubating with cycloheximide (100 μg/ml) to arrest polyribosome migration, five different cell lines (normal or fragile X) were pooled and lysed. After centrifugation, samples were fractionated by bottom displacement by the use of a gradient fractionator (ISCO) with the ribosomal profile monitored at OD_{254}.

RNA Isolation and Oligonucleotide Array Expression Analysis

In immunoprecipitation experiments, RNA from precleared input lysate was isolated with Trizol reagent (GIBCO-BRL) and the RNeasy Mini Kit (QIAGEN). Immunoprecipitated RNA from the brains of both wt and *Fmr1* KO mice was phenol/chloroform extracted and ethanol precipitated. To isolate the RNA from polyribosomes, phenol/chloroform extraction and ethanol precipitation were performed, and the RNA was isolated with the RNeasy Mini Kit (QIAGEN). In addition, total RNA from whole cells treated with cycloheximide was isolated with RNeasy Mini Kit (QIAGEN).

The cRNA "targets" were generated following manufactural instructions (www.affymetrix.com). In immunoprecipitation experiments, one-fifth of the precleared input lysate was used to generate input cRNA. Sixty percent of the wt-IP and the KO-IP RNA was used to generate IP-cRNA targets and was sequentially hybridized to Murine Genome U74 array (subsets A, B, and C) or to Murine 19K array (subsets A, B, and C). Absolute and comparison analyses were performed with Affymetrix Microarray Suite 4.0 software. A recently released mask file to exclude uninformative antisense probe sets from the MG-U74 analyses was applied (www.affymetrix.com). The wt-IP RNA was compared to the KO-IP RNA baseline (scale factor 1, normalization 1). The data was filtered for probe sets "present" and "increased" in wt-IP RNA with a +4.0-fold change or greater. This data was further filtered by comparing wt-IP RNA to the input RNA baseline (scale factor 150, normalization 1), selecting for probe sets present and increased in wt-IP RNA with a +4.0-fold change or greater. Mu19K data comparisons of wt-IP versus the input RNA were performed using the same parameters. In polyribosomal mRNA profile analysis, cRNAs generated from polyribosomal fractions and total mRNA were hybridized to Human 35K (Hu35K) arrays. All the arrays were scaled to an average intensity of 500 and analyzed independently using Affymetrix Microarray Suite 4.0 software. The dendrogram was generated using GENECLUSTER, as described (Eisen et al., 1998).

cDNA Synthesis, RT-PCR, and LightCycler Real-Time PCR

The first strand cDNA was generated by reverse transcription with oligo dT primer or random hexamers. The ^{32}P-labeled UTP first strand cDNA was analyzed via surface tension agarose gel electrophoresis. In RT-PCR analysis, 1 μl of the RT reaction was used in a 27 cycle PCR reaction for each target gene, and products were analyzed by agarose gel electrophoresis. To quantify the mRNA levels with the LightCycler (Roche Molecular Biochemicals), aliquots of first-stranded cDNA were amplified, and real-time fluorimetric intensity of SYBR green I was monitored. The ratio of different samples was calculated by LightCycler Data Analysis Software (Roche Molecular Biochemicals) (see supplemental data).

RNA Slot Blotting

Total RNA (0.5 μg) from normal or fragile X whole cell lysates and the same proportion of RNA from each fraction were used for RNA blotting with gene-specific cDNA probes (see supplemental data).

Acknowledgments

The authors are grateful to F. Zhang, E. Torre, K. Beauregard, T. Johnson, T. Rosser, and J. Clark for assistance. This work was supported, in part, by National Institutes of Health grants RO1 NS34389 (R.B.D.), RO1 HD40647 (J.C.D.), R37 HD20521 and PO1 HD35576 (S.T.W.), by an Irma T. Hirschl Career Scientist Award (R.B.D.), and by a FRAXA Foundation Research Award (J.C.D.). S.T.W. is an investigator, and P.J. and S.C. are associates of the Howard Hughes Medical Institute.

Received June 26, 2001; revised October 4, 2001.

References

The Dutch-Belgian Fragile X Consortium. (1994). Fmr1 knockout mice: a model to study fragile X mental retardation. Cell *78*, 23–33.

Aravamudan, B., Fergestad, T., Davis, W.S., Rodesch, C.K., and Broadie, K. (1999). Drosophila UNC-13 is essential for synaptic transmission. Nat. Neurosci. *2*, 965–971.

Ashley, C.T., Jr., Wilkinson, K.D., Reines, D., and Warren, S.T. (1993). FMR1 protein: conserved RNP family domains and selective RNA binding. Science *262*, 563–566.

Augustin, I., Korte, S., Rickmann, M., Kretzschmar, H.A., Sudhof, T.C., Herms, J.W., and Brose, N. (2001). The cerebellum-specific Munc13 isoform Munc13-3 regulates cerebellar synaptic transmission and motor learning in mice. J. Neurosci. *21*, 10–17.

Bardoni, B., Schenck, A., and Mandel, J.L. (1999). A novel RNA-binding nuclear protein that interacts with the fragile X mental retardation (FMR1) protein. Hum. Mol. Genet. *8*, 2557–2566.

Braun, K., and Segal, M. (2000). FMRP involvement in formation of synapses among cultured hippocampal neurons. Cereb. Cortex *10*, 1045–1052.

Brown, V., Small, K., Lakkis, L., Feng, Y., Gunter, C., Wilkinson, K.D., and Warren, S.T. (1998). Purified recombinant FMRP exhibits selective RNA binding as an intrinsic property of the fragile X mental retardation protein. J. Biol. Chem. *273*, 15521–15527.

Caroni, P. (1997). Intrinsic neuronal determinants that promote axonal sprouting and elongation. Bioessays *19*, 767–775.

Ceman, S., Brown, V., and Warren, S.T. (1999). Isolation of an FMRP-associated messenger ribonucleoprotein particle and identification of nucleolin and the fragile X-related proteins as components of the complex. Mol. Cell. Biol. *19*, 7925–7932.

Ceman, S., Nelson, R., and Warren, S.T. (2000). Identification of mouse YB1/p50 as a component of the FMRP-associated mRNP particle. Biochem. Biophys. Res. Commun. *279*, 904–908.

Ceman, S., Zhang, F., Johnson, T., and Warren, S.T. (2001). Development and characterization of antibodies that immunoprecipitate the FMR1 protein. In Methods in Molecular Medicine-Neurogenetics: Methods and Protocols, N.T. Potter, ed. (Totowa, NJ: Human Press, Inc.), in press.

Darnell, J.C., Jensen, K.B., Jin, P., Brown, V., Warren, S.T., and Darnell, R.B. (2001) Fragile X mental retardation protein targets G quartet mRNAs important for neuronal function. Cell *107*, 489–499.

De Boulle, K., Verkerk, A.J., Reyniers, E., Vits, L., Hendrickx, J., Van Roy, B., Van den Bos, F., de Graaff, E., Oostra, B.A., and Willems, P.J. (1993). A point mutation in the FMR-1 gene associated with fragile X mental retardation. Nat. Genet. *3*, 31–35.

Eberhart, D.E., Malter, H.E., Feng, Y., and Warren, S.T. (1996). The fragile X mental retardation protein is a ribonucleoprotein containing both nuclear localization and nuclear export signals. Hum. Mol. Genet. *5*, 1083–1091.

Edelmann, W., Zervas, M., Costello, P., Roback, L., Fischer, I., Hammarback, J.A., Cowan, N., Davies, P., Wainer, B., and Kucherlapati, R. (1996). Neuronal abnormalities in microtubule-associated protein 1B mutant mice. Proc. Natl. Acad. Sci. USA *93*, 1270–1275.

Eisen, M.B., Spellman, P.T., Brown, P.O., and Botstein, D. (1998). Cluster analysis and display of genome-wide expression patterns. Proc. Natl. Acad. Sci. USA *95*, 14863–14868.

El-Husseini, A.E., Schnell, E., Chetkovich, D.M., Nicoll, R.A., and Bredt, D.S. (2000). PSD-95 involvement in maturation of excitatory synapses. Science *290*, 1364–1368.

Feng, Y., Absher, D., Eberhart, D.E., Brown, V., Malter, H.E., and Warren, S.T. (1997a). FMRP associates with polyribosomes as an mRNP, and the I304N mutation of severe fragile X syndrome abolishes this association. Mol. Cell *1*, 109–118.

Feng, Y., Gutekunst, C.A., Eberhart, D.E., Yi, H., Warren, S.T., and Hersch, S.M. (1997b). Fragile X mental retardation protein: nucleocytoplasmic shuttling and association with somatodendritic ribosomes. J. Neurosci. *17*, 1539–1547.

Frey, D., Laux, T., Xu, L., Schneider, C., and Caroni, P. (2000). Shared and unique roles of CAP23 and GAP43 in actin regulation, neurite outgrowth, and anatomical plasticity. J. Cell Biol. *149*, 1443–1454.

Hinton, V.J., Brown, W.T., Wisniewski, K., and Rudelli, R.D. (1991). Analysis of neocortex in three males with the fragile X syndrome. Am. J. Med. Genet. *41*, 289–294.

Ishizuka, T., Saisu, H., Odani, S., Kumanishi, T., and Abe, T. (1999). Distinct regional distribution in the brain of messenger RNAs for the two isoforms of synaphin associated with the docking/fusion complex. Neuroscience *88*, 295–306.

Jackson, C.L., and Casanova, J.E. (2000). Turning on ARF: the Sec7 family of guanine-nucleotide exchange factors. Trends Cell Biol. *10*, 60–67.

Jin, P., and Warren, S.T. (2000). Understanding the molecular basis of fragile X syndrome. Hum. Mol. Genet. *9*, 901–908.

Keene, J.D. (2001). Ribonucleoprotein infrastructure regulating the flow of genetic information between the genome and the proteome. Proc. Natl. Acad. Sci. USA *98*, 7018–7024.

Khandjian, E.W., Corbin, F., Woerly, S., and Rousseau, F. (1996). The fragile X mental retardation protein is associated with ribosomes. Nat. Genet. *12*, 91–93.

Laggerbauer, B., Ostareck, D., Keidel, E.M., Ostareck-Lederer, A., and Fischer, U. (2001). Evidence that fragile X mental retardation protein is a negative regulator of translation. Hum. Mol. Genet. *10*, 329–338.

Li, Z., Zhang, Y., Ku, L., Wilkinson, K.D., Warren, S.T., and Feng, Y. (2001). The fragile X mental retardation protein inhibits translation via interacting with mRNA. Nucleic Acids Res. *29*, 2276–2283.

Mayer, G., Blind, M., Nagel, W., Bohm, T., Knorr, T., Jackson, C.L., Kolanus, W., and Famulok, M. (2001). Controlling small guanine-nucleotide-exchange factor function through cytoplasmic RNA intramers. Proc. Natl. Acad. Sci. USA *98*, 4961–4965.

Naeve, G.S., Ramakrishnan, M., Kramer, R., Hevroni, D., Citri, Y., and Theill, L.E. (1997). Neuritin: a gene induced by neural activity and neurotrophins that promotes neuritogenesis. Proc. Natl. Acad. Sci. USA *94*, 2648–2653.

Neeb, A., Koch, H., Schurmann, A., and Brose, N. (1999). Direct interaction between the ARF-specific guanine nucleotide exchange factor msec7-1 and presynaptic Munc13-1. Eur. J. Cell Biol. *78*, 533–538.

Nimchinsky, E.A., Oberlander, A.M., and Svoboda, K. (2001). Abnormal development of dendritic spines in FMR1 knock-out mice. J. Neurosci. *21*, 5139–5146.

Oberle, I., Rousseau, F., Heitz, D., Kretz, C., Devys, D., Hanauer, A., Boue, J., Bertheas, M.F., and Mandel, J.L. (1991). Instability of a 550-base pair DNA segment and abnormal methylation in fragile X syndrome. Science *252*, 1097–1102.

Paschen, W., Blackstone, C.D., Huganir, R.L., and Ross, C.A. (1994). Human GluR6 kainate receptor (GRIK2): molecular cloning, expression, polymorphism, and chromosomal assignment. Genomics *20*, 435–440.

Query, C.C., Bentley, R.C., and Keene, J.D. (1989). A common RNA recognition motif identified within a defined U1 RNA binding domain of the 70K U1 snRNP protein. Cell *57*, 89–101.

Satoh, K., Yanai, H., Senda, T., Kohu, K., Nakamura, T., Okumura, N., Matsumine, A., Kobayashi, S., Toyoshima, K., and Akiyama, T. (1997). DAP-1, a novel protein that interacts with the guanylate kinase-like domains of hDLG and PSD-95. Genes Cells *2*, 415–424.

Schenck, A., Bardoni, B., Moro, A., Bagni, C., and Mandel, J.L. (2001). A highly conserved protein family interacting with the fragile X mental retardation protein (FMRP) and displaying selective interactions with FMRP-related proteins FXR1P and FXR2P. Proc. Natl. Acad. Sci. USA *98*, 8844–8849.

Siomi, H., Choi, M., Siomi, M.C., Nussbaum, R.L., and Dreyfuss, G. (1994). Essential role for KH domains in RNA binding: impaired RNA binding by a mutation in the KH domain of FMR1 that causes fragile X syndrome. Cell *77*, 33–39.

Siomi, H., Siomi, M.C., Nussbaum, R.L., and Dreyfuss, G. (1993). The protein product of the fragile X gene, FMR1, has characteristics of an RNA-binding protein. Cell *74*, 291–298.

Sung, Y.J., Conti, J., Currie, J.R., Brown, W.T., and Denman, R.B. (2000). RNAs that interact with the fragile X syndrome RNA binding protein FMRP. Biochem. Biophys. Res. Commun. *275*, 973–980.

Sutcliffe, J.S., Nelson, D.L., Zhang, F., Pieretti, M., Caskey, C.T., Saxe, D., and Warren, S.T. (1992). DNA methylation represses FMR-1 transcription in fragile X syndrome. Hum. Mol. Genet. *1*, 397–400.

Takeuchi, M., Hata, Y., Hirao, K., Toyoda, A., Irie, M., and Takai, Y. (1997). SAPAPs. A family of PSD-95/SAP90-associated proteins localized at postsynaptic density. J. Biol. Chem. *272*, 11943–11951.

Tamanini, F., Meijer, N., Verheij, C., Willems, P.J., Galjaard, H., Oostra, B.A., and Hoogeveen, A.T. (1996). FMRP is associated to the ribosomes via RNA. Hum. Mol. Genet. *5*, 809–813.

Tenenbaum, S.A., Carson, C.C., Lager, P.J., and Keene, J.D. (2000). Identifying mRNA subsets in messenger ribonucleoprotein complexes by using cDNA arrays. Proc. Natl. Acad. Sci. USA *97*, 14085–14090.

Verkerk, A.J., Pieretti, M., Sutcliffe, J.S., Fu, Y.-H., Kuhl, D.P.A., Pizutti, A., Reiner, O., Richards, S., Victoria, M.F., Zhang, F., et al. (1991). Identification of a gene (*FMR-1*) containing a CGG repeat coincident with a breakpoint cluster region exhibiting length variation in fragile X syndrome. Cell *65*, 905–914.

Weiler, I.J., Irwin, S.A., Klintsova, A.Y., Spencer, C.M., Brazelton, A.D., Miyashiro, K., Comery, T.A., Patel, B., Eberwine, J., and Greenough, W.T. (1997). Fragile X mental retardation protein is translated near synapses in response to neurotransmitter activation. Proc. Natl. Acad. Sci. USA *94*, 5395–5400.

Zhang, Y., O'Connor, J.P., Siomi, M.C., Srinivasan, S., Dutra, A., Nussbaum, R.L., and Dreyfuss, G. (1995). The fragile X mental retardation syndrome protein interacts with novel homologs FXR1 and FXR2. EMBO J. *14*, 5358–5366.